Cancer Chemother Pharmacol (2003) 52: 417–423
DOI 10.1007/s00280-003-0674-0

ORIGINAL ARTICLE

**Patrick Thompson · Frank Balis · Baruti M. Serabe
Stacey Berg · Peter Adamson · Renee Klenke
Alberta Aiken · Roger Packer · Daryl J. Murry
Regina Jakacki · Susan M. Blaney**

Pharmacokinetics of phenylacetate administered as a 30-min infusion in children with refractory cancer

Published online: 15 July 2003

Abstract *Purpose*: Phenylacetate (PAA), a deaminated metabolite of phenylalanine, suppresses tumor growth and induces differentiation in preclinical tumor models. We performed a pharmacokinetic study, as part of a phase I trial, of PAA in children with refractory cancer. *Methods*: PAA was administered as a 30-min i.v. infusion at a dose of 1.8 or 2.5 g/m^2. Serial plasma samples were collected for up to 24 h after the end of the infusion in 27 children. The concentrations of PAA and its inactive metabolite, phenylacetylglutamine (PAG), were measured using a reverse-phase high-performance liquid chromatography assay with ultraviolet detection. *Results*: PAA and PAG concentrations were best described by a two-compartment model (one compartment for each compound) with capacity-limited conversion of PAA to PAG. The half-life of PAA was 55 ± 18 min at the 1.8 g/m^2 dose and 77 ± 22 min at the 2.5 g/m^2 dose. The half-life of PAG was 112 ± 53 min at the 1.8 g/m^2 dose and 135 ± 75 min at the 2.5 g/m^2 dose. The clearance of PAA was 66 ± 33 ml/min per m^2 at the 1.8 g/m^2 dose and 60 ± 24 ml/min per m^2 at the 2.5 g/m^2 dose. The Michaelis-Menten constants describing the conversion of PAA to PAG in the model (V_m and K_m) were (means ± SD) 18.4 ± 13.8 mg/m^2 per min and 152 ± 155 μg/ml, respectively. The volumes of distribution for PAA and PAG ($V_{d\text{-}PAA}$ and $V_{d\text{-}PAG}$) were 7.9 ± 3.4 l/m^2 and 34.4 ± 16.1 l/m^2, respectively. The first-order elimination rate constant for PAG ($k_{e\text{-}PAG}$) was 0.0091 ± 0.0039 min^{-1}. *Conclusions*: The capacity-limited conversion of PAA to PAG has important implications for the dosing of PAA, and the pharmacokinetic model described here may be useful for individualizing the infusion rate of the drug in future clinical trials.

Keywords Pharmacokinetic · Phenylacetate · Pediatric · Phenylacetylglutamine

This work was supported in part by the National Institutes of Health (M01-RR00188), and the General Clinical Research Center, Baylor College of Medicine.

P. Thompson
Department of Pediatrics,
Baylor College of Medicine, Houston, TX, USA

F. Balis · P. Adamson · A. Aiken
Pediatric Oncology Branch,
National Cancer Institute, Bethesda, MD, USA

B. M. Serabe · S. Berg · R. Klenke · D. J. Murry · S. M. Blaney
Texas Children's Cancer Center,
Baylor College of Medicine, Houston, TX, USA

R. Packer
Department of Hematology-Oncology,
Children's National Medical Center, Washington, DC, USA

R. Jakacki
Division of Hematology-Oncology,
Riley Hospital for Children, Indianapolis, IN, USA

S. M. Blaney (✉)
Texas Children's Cancer Center, 6621 Fannin, MC 3-3320,
Houston, TX 77030, USA
E-mail: sblaney@txccc.org
Tel.: +1-832-8221482
Fax: +1-832-8254299

Present address: B. M. Serabe
Medcenter One Health Systems, Bismarck, ND, USA

Present address: P. Adamson
Children's Hospital Philadelphia, Philadelphia, PA, USA

Present address: D. J. Murry
Purdue University, Indianapolis, IN, USA

Present address: R. Jakacki
Children's Hospital Pittsburgh, Pittsburgh, PA, USA

Introduction

Phenylacetate (PAA), a deaminated metabolite of phenylalanine, is normally present in the mammalian circulation in micromolar concentrations [1]. In preclinical studies, exposure to millimolar concentrations of PAA can induce tumor cytostasis and differentiation in a variety of tumor cell lines, including malignant gliomas,

hormone-refractory prostate carcinoma, malignant melanoma, neuroblastoma, lymphoblastic leukemia, and adenocarcinomas of the breast, colon and lung [2, 3, 4, 5, 6, 7, 8]. Postulated mechanisms for PAA-induced cytostasis and tumor differentiation include: alterations in lipid metabolism, regulation of gene expression through DNA hypomethylation and transcriptional activation, inhibition of protein isoprenylation, and glutamine depletion [5]. These unique mechanisms of action, combined with preclinical evidence of antitumor activity, have led to the clinical development of PAA as a potential anticancer agent.

PAA has been administered in high doses to children with hyperammonemia due to inborn errors of urea synthesis [9, 10]. PAA is eliminated by conjugation with glutamine to yield phenylacetylglutamine (PAG), which is subsequently excreted in the urine [11, 12]. Mobilization of glutamine-associated nitrogen is believed to lead to the observed improvements in hyperammonemia. In children with urea cycle defects who received PAA doses of 2 mmol/kg (about 8 g/m^2), PAA elimination was found to follow first-order kinetics with a $t_{1/2}$ of 254 min [10]. In adults who received PAA as an anticancer agent, the pharmacokinetic behavior of PAA after administration of a 30-min bolus infusion was described by a one-compartment model, with capacity-limited elimination [13, 14].

In the present study, we investigated the pharmacokinetics of PAA in children with refractory cancers who received a 30-min infusion of PAA as part of a phase I clinical trial. We developed a pharmacokinetic model that describes the disposition of PAA and the formation and elimination of the metabolite, PAG.

Patients and methods

Patient eligibility

Children between 2 and 21 years of age with histologically confirmed cancer refractory to standard therapy or with surgically inoperable plexiform neurofibromas with the potential to cause significant morbidity were eligible for the study. Other eligibility criteria included: (a) adequate renal, hepatic, pulmonary and cardiovascular function; (b) recovery from the toxic effects of all prior therapy; (c) an ECOG performance status ≤ 2; (d) a life expectancy of at least 8 weeks; and (e) the presence of a permanently indwelling central venous access device. Patients were excluded if they: (a) were pregnant or lactating; (b) had a significant systemic illness; (c) had a pre-existing grade 2 neurocortical toxicity; or (d) had an amino aciduria or organic acidemia. Patients receiving dexamethasone were required to be on a stable or decreasing dose for at least 2 weeks prior to study entry. Informed consent was obtained from the patient or parent in accordance with individual institutional policies prior to entry onto this study. Toxicities were evaluated using version 1 of the NCI Common Toxicity Criteria [15]. Table 1 summarizes the characteristics of patients enrolled in the study.

Dosage and drug administration

PAA was supplied by the Investigational Drug Branch, National Cancer Institute (Bethesda, Md.) as a 50% (500 mg/ml) solution of sodium PAA in sterile water. The appropriate dose of the drug was diluted in 30 ml sterile water. PAG for HPLC standards was supplied by Elan Pharmaceutical and Research Company (Gainesville, Ga.).

In order to characterize PAA pharmacokinetics, a 30-min i.v. infusion was administered 1 day prior to the start of a 28-day continuous infusion. The initial i.v. bolus dose was 1.8 g/m^2 ($n = 13$), which was approximately 80% of the bolus dose administered in phase I clinical trials in adults. The dose was subsequently increased to 2.5 g/m^2 ($n = 14$) due to the rapid plasma elimination of PAA and lack of toxicity at the lower dose. The continuous i.v. dose received by patients varied from 7 to 12 g/m^2 per day. The results of the phase I clinical trial will be reported separately.

Table 1 Patient demographics

Total number of patients	27
Age (years)	
Median	10
Range[a]	1.4–20
Weight (kg)	
Mean ± SD	36 ± 24
Range	9.9–93.5
Body surface area (m^2)	
Mean ± SD	1.17 ± 0.47
Range	0.48–2.3

[a]Two patients < 2 years of age enrolled by special exemption

Pharmacokinetic studies

Blood samples were obtained prior to the start of the infusion, at 15 min during the infusion, at the end of the infusion, and at 5, 15, 30 min, and 1, 2, 4, 6, 8, 10 and 24 h following the completion of the infusion. Samples were drawn from a site separate from the infusion site. Blood samples were collected into heparinized tubes, placed on ice, and centrifuged to separate the plasma. Plasma was stored at −80°C until the day of analysis.

Analytical method

Plasma PAA and PAG concentrations were measured using a previously reported reverse-phase high-pressure liquid chromatograph (HPLC) assay with minor modification [13]. Plasma (200 µl) was transferred to a 1.7-ml Eppendorf tube (Brinkmann Instruments, Westbury, N.Y.). Protein was precipitated by adding 180 µl 100% methanol (EM Science, Gibbstown, N.J.) and 20 µl 40% zinc sulfate (Sigma Chemical Company, St. Louis, Mo.). The sample was vortexed, centrifuged (4500 *g* for 5 min) and the supernatant (150 µl) transferred to an autosampler vial maintained at 10°C until HPLC injection. The injection volume was 20 µl. Recovery was 85 ± 7.7% for PAA and 90 ± 16% for PAG.

The HPLC system consisted of a Waters model 600 automated gradient controller, a Waters programmable ultraviolet multiwavelength detector model 490E and a Waters model 717 autosampler (Waters Corporation, Milford, Mass.). The analytical column was a Waters C-18 Novapak, 3.9×300 mm (Millipore Corporation, Milford, Mass.) maintained at 60°C with a column heater. Mobile phase A was 5% acetonitrile acidified with 0.005 *M* phosphoric acid and mobile phase B was acetonitrile acidified with 0.005 *M* phosphoric acid. A linear gradient from 100% A to 70% A/30%B over 20 min was used. The total flow rate was 1 ml/min. The column was then washed with 50% A/50% B for 10 min and allowed to equilibrate with 100% A for 10 min between injections. The total run time was 40 min. PAA and PAG were monitored at 208 nm. Retention times for PAA and PAG were 18 and 12.5 min, respectively.

Standard curves in donor plasma were prepared for each HPLC run. Standard curves were linear over the ranges 5 to 750 µg/ml for PAA and 10 to 750 µg/ml for PAG. The interday coefficient of variation was less than 12%.

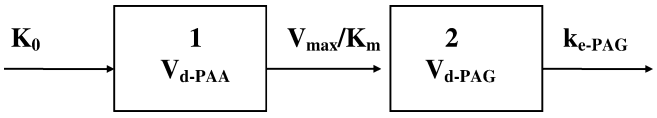

Fig. 1 Capacity-limited model for the pharmacokinetic disposition of PAA in children with refractory cancer. There are separate compartments for PAA and PAG and capacity-limited conversion of PAA to PAG. *Box 1* represents the PAA compartment and *box 2* the PAG compartment. K_0 represents the infusion of PAA. V_{max} and K_m are the Michaelis-Menten constants for capacity-limited kinetics and $k_{e\text{-}PAG}$ is the first-order elimination rate constant for PAG. $V_{d\text{-}PAA}$ and $V_{d\text{-}PAG}$ represent the volumes of distribution for PAA and PAG

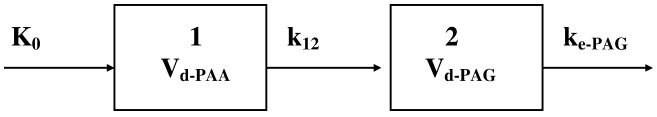

Fig. 2 First-order model for the pharmacokinetic disposition of PAA in children with refractory cancer. There are separate compartments for PAA and PAG and capacity-limited conversion of PAA to PAG. *Box 1* represents the PAA compartment and *box 2* the PAG compartment. K_0 represents the infusion of PAA. k_{12} is the first-order rate constant for the conversion of PAA to PAG, and $k_{e\text{-}PAG}$ is the first-order elimination rate constant for PAG. $V_{d\text{-}PAA}$ and $V_{d\text{-}PAG}$ represent the volumes of distribution for PAA and PAG

Pharmacokinetic and statistical analysis

Pharmacokinetic sampling was carried out in 27 patients. Non-compartmental methods were used to calculate the area under the concentration versus time curve (AUC), the model-independent total body clearance (Cl_{TB}), and model-independent steady-state volume of distribution (Vd_{SS}) for PAA. AUC was also determined for PAG. For both compounds the AUC was derived by the linear trapezoidal method and extrapolated to infinity by adding the quotient of the final plasma concentration divided by the terminal rate constant. For PAA the Cl_{TB} was determined by dividing the dose by the AUC, and the Vd_{SS} for PAA was calculated using the area under the moment curve. The terminal half-lives for PAA and PAG were calculated from the slope of the best-fit line through the last three or four data points.

The pharmacokinetic models depicted in Figs. 1 and 2 were fitted to the plasma concentration versus time data from the individual patient data sets using MLAB software (Civilized Software, Bethesda, Md.). Both models incorporated single compartments for PAA and PAG, with either first-order or capacity-limited conversion of PAA to PAG, and subsequent first-order elimination for PAG.

Model with capacity-limited conversion of PAA to PAG

The differential equations that describe the model are as follows:

$$\frac{dX_1}{dt} = Infusion - \frac{V_{max}X_1}{K^*_m + X_1} \qquad \frac{dX_2}{dt} = \frac{V_{max}X_1}{K^*_m + X_1} - K_e X_2$$

$$K_m = K^*_m \cdot V_1 \qquad C_1 = \frac{X_1}{V_1} \qquad C_2 = \frac{X_2}{V_2}$$

Where:

X_1	Amount of PAA
X_2	Amount of PAG
C_1	Concentration of PAA
C_2	Concentration of PAG
V_1	Volume of distribution PAA
V_2	Volume of distribution PAG
K^*_m	Half-saturation constant (Michaelis-Menten parameter) expressed on a mass basis
V_{max}	Maximum velocity (Michaelis-Menten parameter) expressed on a mass basis
K_m	Half-saturation constant expressed on a concentration basis
K_e	First-order elimination rate constant for PAG

Model with first-order conversion of PAA to PAG

The differential equations that describe the model are as follows:

$$\frac{dX_1}{dt} = Infusion - k_{12}X_1 \qquad \frac{dX_2}{dt} = k_{12}X_1 - K_e X_2$$

$$C_1 = \frac{X_1}{V_1} \qquad C_2 = \frac{X_2}{V_2}$$

Where:

X_1	Amount of PAA
X_2	Amount of PAG
C_1	Concentration of PAA
C_2	Concentration of PAG
V_1	Volume of distribution PAA
V_2	Volume of distribution PAG
k_{12}	First-order rate constant for conversion of PAA to PAG
k_e	First-order elimination rate constant for PAG

The completed model fits were compared in two ways: (1) by evaluating the sum of residual squared error (weighted by the inverse concentration squared), and (2) by calculating the Akaike Information Criteria [16].

The capacity-limited and first-order kinetic models were further evaluated by comparing their ability to predict the steady-state concentrations observed in the continuous i.v. infusions. The model parameters derived for each patient from the bolus data were used to predict the steady-state levels of PAA and PAG for the continuous infusion.

Since most of the children enrolled in this study had primary CNS tumors, additional analysis was done retrospectively to attempt to determine whether dexamethasone or anticonvulsants, medications that this patient population commonly receives, interfered with the metabolism or clearance of PAA. To evaluate this issue pharmacokinetic parameters were compared between the group receiving medication and the group that was not. A two-sided *t*-test was performed to determine significance.

Results

Model-independent pharmacokinetic parameters

Model-independent pharmacokinetic parameters for PAA and PAG are provided in Table 2 for both bolus dose levels tested.

Model fit: comparison of capacity-limited kinetics and first-order kinetics

Representative concentration versus time curves of model-predicted and actual PAA and PAG concentrations following administration of either a 1.8 g/m^2 or a 2.5 g/m^2 30-min i.v. infusion are shown in Fig. 3. The figure shows experimental data for two typical patients and model fits generated with both the capacity-limited and first-order pharmacokinetics. Overall the capacity-

Table 2 Model-independent PAA and PAG pharmacokinetic parameters for both doses tested. Values are means ± SD

	Parameter	Units	Dose (g/m^2)	
			1.8	2.5
PAA	Maximum concentration	μg/ml	253 ± 51	359 ± 121
	AUC	μg·min/ml	32,200 ± 12,500	49,800 ± 23,800
	Cl_{TB}	$ml/min/m^2$	66.4 ± 33.4	59.9 ± 24.0
	$V_{d\text{-}ss}$	l/m^2	5.3 ± 1.1	6.6 ± 2.9
	$t_{1/2}$	min	55 ± 19	77 ± 22
PAG	Maximum concentration	μg/ml	55 ± 18	67 ± 29
	AUC	μg·min/ml	18,800 ± 12,000	24,000 ± 12,700
	$t_{1/2}$	min	112 ± 53	135 ± 75

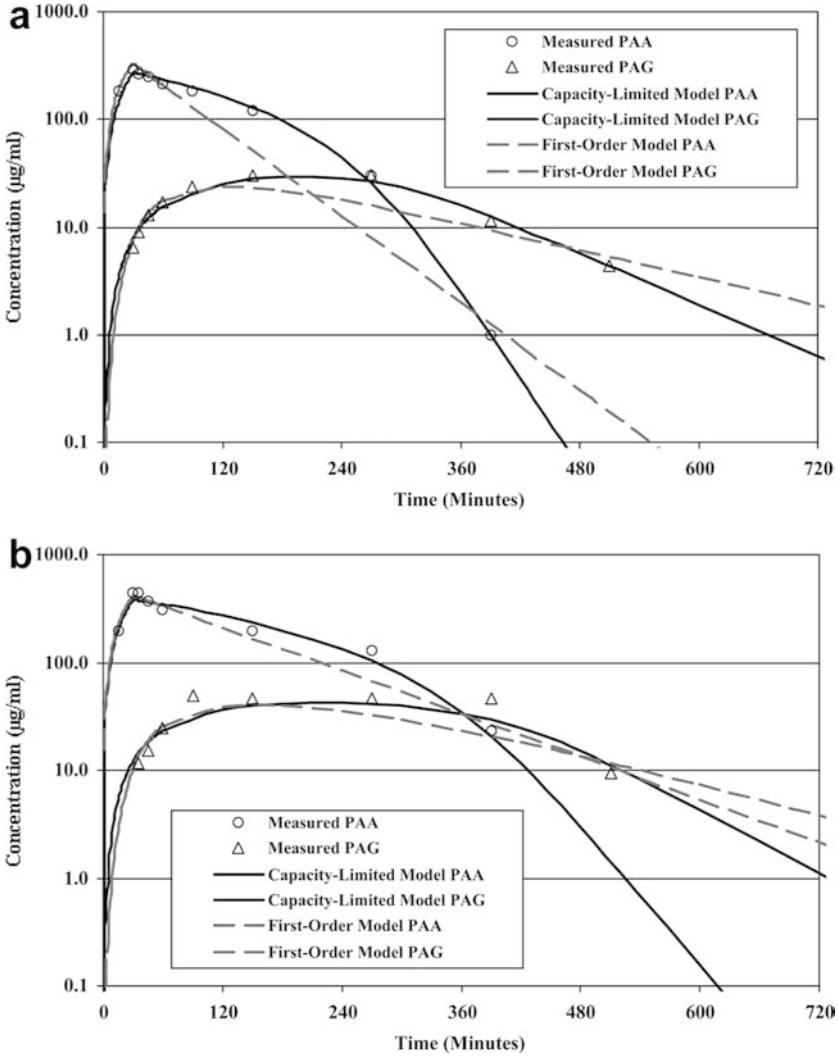

Fig. 3a, b Serum concentrations of PAA (○) and PAG (△) are shown for representative patients following (**a**) a 1.8-g/m^2 i.v. bolus of PAA over 30 min, and (**b**) a 2.5-g/m^2 i.v. bolus over 30 min. The *solid lines* represent the model fit with capacity-limited kinetics, and the *dashed lines* represent the model fit with first-order kinetics

limited model fitted the patient data very well, with a mean r^2 of 0.939 ± 0.082.

Comparison to the first-order model showed that capacity-limited kinetics provided a lower sum of residual squares in 22 of 27 patients and a lower AIC in 20 of 27 patients. Additionally, for three of the seven patients whose concentration versus time data were fitted best by a first-order model, it was difficult to fit the experimental data to the capacity-limited kinetic model because there were fewer late data points (concentrations at 4 h post-infusion were below the lower limit of quantitation for the assay).

Model-dependent pharmacokinetic parameters

Tables 3 and 4 show the mean and median pharmacokinetic parameters determined from this study for the

Table 3 Model-dependent PAA and PAG pharmacokinetic parameters (results based on patients enrolled at both doses and results normalized on body surface area and mass)

	Parameter	Units	Mean	Median	SD	CV (%)
Area basis	K_m	mg/l	152	99.0	155	101.9
	V_{max}	mg/m^2/min	18.4	13.8	13.8	74.8
	$k_{e\text{-}PAG}$	min^{-1}	0.0091	0.0087	0.0039	43.2
	$V_{d\text{-}PAA}$	l/m^2	7.97	6.74	3.29	41.2
	$V_{d\text{-}PAG}$	l/m^2	35.0	31.9	16.0	45.6
Mass basis	K_m	mg/kg	33.0	25.3	23.3	70.5
	V_{max}	mg/kg/h	34.9	24.1	22.8	65.2
	$k_{e\text{-}PAG}$	h^{-1}	0.54	0.52	0.24	43.2
	$V_{d\text{-}PAA}$	l/kg	0.27	0.23	0.13	48.4
	$V_{d\text{-}PAG}$	l/kg	1.15	1.06	0.56	48.7

Table 4 Model-dependent PAA and PAG pharmacokinetic parameters at each dose tested

Dose (g/m^2)	Parameter	Units	Mean	Median	SD	CV (%)
1.8	K_m	mg/l	142	89.7	155	109.2
	V_{max}	mg/m^2/min	18.3	13.5	14.7	80.3
	$k_{e\text{-}PAG}$	min^{-1}	0.0087	0.0089	0.0041	47.1
	$V_{d\text{-}PAA}$	l/m^2	6.84	6.43	1.25	18.3
	$V_{d\text{-}PAG}$	l/m^2	35.3	39.1	9.2	26.1
2.5	K_m	mg/l	161	118	144	89.4
	V_{max}	mg/m^2/min	18.6	15.0	12.8	68.8
	$k_{e\text{-}PAG}$	min^{-1}	0.0094	0.0084	0.0038	40.4
	$V_{d\text{-}PAA}$	l/m^2	9.02	6.97	4.13	45.8
	$V_{d\text{-}PAG}$	l/m^2	34.7	28.3	20.3	58.5

capacity-limited model. The results are expressed in two sets of units to facilitate comparison with other published data on PAA [13, 14]. Using the same units as previously published adult data, the model-dependent PAA pharmacokinetic parameters (K_m, V_{max} and $V_{d\text{-}PAA}$) in children were 152 ± 155 μg/ml, 35.0 ± 16 mg/kg per h, and 0.27 ± 0.13 l/kg, respectively. These values are similar to previously reported parameters in adults: K_m 105 ± 44.5 μg/ml, V_{max} 24.1 ± 5.2 mg/kg per h, and $V_{d\text{-}PAA}$ 19.2 ± 3.3 l [13]. Assuming a 70-kg adult, the PAA volume of distribution for adults is approximately 0.27 ± 0.047 l/kg.

As shown in Table 3, the variabilities of V_{max} and K_m are large. However, the variability decreased if the seven data sets which were fitted better by the first-order model than the capacity-limited model were disregarded. Based on the subset of 20 patients in whom the capacity-limited model was superior, K_m was 92.9 ± 42.4 μg/ml and V_{max} 26.9 ± 12.2 mg/kg per h. Other model-dependent parameters for this subset of patients did not significantly differ from the mean values for the complete study group.

Estimation of continuous infusion drug levels using bolus pharmacokinetic parameters

Both the capacity-limited and first-order kinetic models were used to predict steady-state levels for patients receiving continuous i.v. infusions. This was done by using the model parameters for each patient derived from the bolus data to predict the steady-state levels of PAA and PAG during the continuous infusion. Figures 4 and 5 show the predicted PAA levels for both models plotted against the average measured steady-state levels for patients receiving continuous infusions of 7 and 9 g/m^2 per day, respectively. Each data point represents one patient and the 45° line represents perfect agreement between the model and the data.

Effect of concurrent medications

Since most of the children enrolled in this study had primary CNS tumors, we retrospectively attempted to determine whether dexamethasone or anticonvulsants, medications that this patient population commonly receives, interfered with the metabolism or clearance of PAA. There were no statistically significant relationships between concomitant administration of dexamethasone ($n = 12$), phenytoin ($n = 4$), or both ($n = 2$) and the AUC for PAA or PAG. Likewise, there were no correlations between concomitant administration of these medications and CL_{TB} for PAA. However, potential interactions may not have been detected because of the relatively small number of patients who were receiving concomitant anticonvulsants.

Discussion

Pharmacokinetics of PAA following bolus dose administration

Early studies of the plasma pharmacokinetics of PAA following bolus dose administration of 2 mmol/kg (about 270 mg/kg or 8 g/m^2) performed in children with

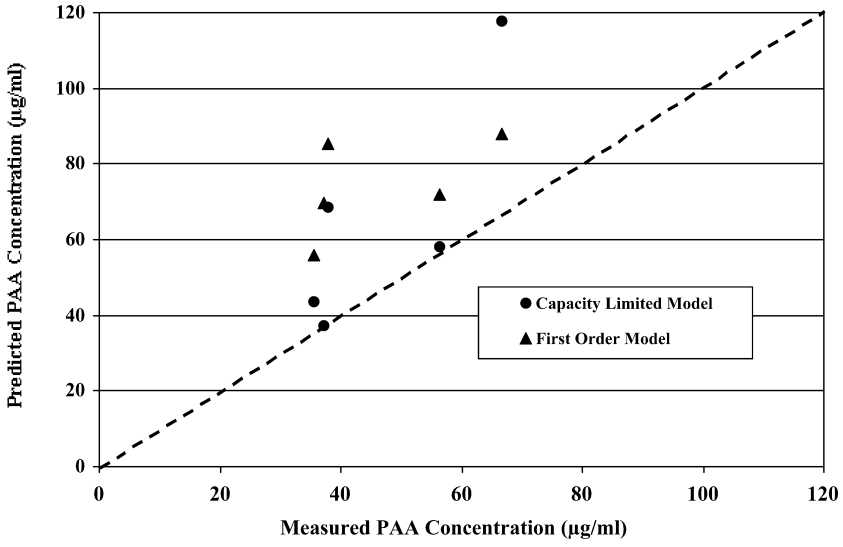

Fig. 4 Predicted steady-state concentrations of PAA using the capacity-limited (●) and first-order model (▲) plotted against the average measured steady-state concentration for patients receiving a continuous i.v. infusion of PAA at 7 g/m^2 per day

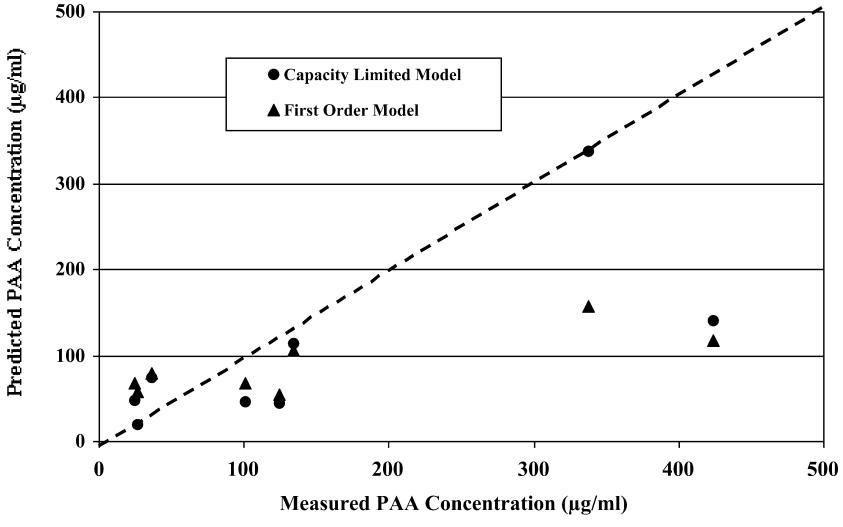

Fig. 5 Predicted steady-state concentrations of PAA using the capacity-limited (●) and first-order model (▲) plotted against the average measured steady-state concentration for patients receiving a continuous i.v. infusion of PAA at 9 g/m^2 per day

disorders of urea cycle synthesis showed first-order drug elimination [10]. The nonlinear nature of PAA elimination may not have been recognized because relatively few post-infusion plasma samples were analyzed for PAA. However, the data from this pediatric study suggest that PAA elimination is nonlinear because the capacity-limited model described the data better than the first-order elimination model in 20 of 27 patients, based on residual sum of squares and AIC. In addition, model-dependent parameters derived from this study are consistent with those published for capacity-limited kinetics of PAA in adults (K_m 105 ± 44.5 µg/ml, V_{max} 24.1 ± 5.2 mg/kg per h, and $V_{d\text{-}PAA}$ 19.2 ± 3.3 l).

The model-independent parameters calculated for the two PAA dose levels studied are consistent with capacity-limited kinetics. At the higher PAA dose (2.5 g/m^2), the increase in AUC was slightly greater than predicted based on the incremental increase in dose (55% versus 40%) while the clearance was slightly decreased (about 10%). The differences noted were not statistically significant, however, probably because most drug concentrations measured, even at the higher dose level, fell below the K_m (i.e., in the "linear" range of the capacity-limited model). Using the mean capacity-limited model parameters, we would predict that a dose increase from 1.8 g/m^2 to 2.5 g/m^2 would result in a 63% increase in AUC and a 15% decrease in clearance, nearly identical to that actually observed. Thus, the model-independent parameters are consistent with the capacity-limited model proposed.

Pharmacokinetics of continuous PAA infusion

The good agreement between model predictions and measured steady-state levels in patients receiving continuous infusions of PAA supports the value of using models derived from the bolus data. However, the results do not help distinguish which model is most appropriate for PAA pharmacokinetics. As shown in

Figs. 4 and 5, steady-state levels for the 7 g/m^2 per day and 9 g/m^2 per day infusion rates can generally be well predicted using bolus pharmacokinetic parameters with either the capacity-limited or first-order models. For one patient receiving 9 g/m^2 per day, the capacity-limited model was significantly better because it predicted the observed high steady-state level. In general, though, comparison of the two models using the continuous infusion data was limited by the fact that the achieved steady-state levels were typically below the K_m of PAA. Unfortunately, patients receiving the highest doses of the continuous infusion (which in some cases achieved concentrations in excess of the K_m) were enrolled after completion of the bolus study.

Conclusions

We present here the first pharmacokinetic model of PAA to include parameters for the formation and elimination of the metabolite PAG in children with refractory cancer. The overall results of this study suggest that the model most consistent with the experimentally observed pharmacokinetics of PAA includes a capacity-limited conversion of PAA to PAG. Additionally, this study also showed that models developed from bolus pharmacokinetic studies of PAA may be useful in predicting the steady-state levels achieved during a continuous i.v. infusion.

The nonlinear nature of PAA pharmacokinetics and the significant interpatient variability in clearance will present a challenge in making uniform dosing recommendations using traditional dosing schemes that are based on body weight or surface area. Pharmacokinetic and pharmacodynamic studies should be an integral part of future clinical trials in order to maximize the potential therapeutic efficacy and minimize the toxicity of PAA.

References

1. Sandler M, Ruthven CRJ, Goodwin BL, Lee A, Stern GM (1982) Phenylacetic acid in human body fluids: high correlation between plasma and cerebrospinal fluid concentration values. J Neurol Neurosurg Psychol 45:366–368
2. Ram Z, Samid D, Walbridge S, Oshiro E, Viola J, Tao-Cheng J-H, Shack S, Thibault A, Myers C, Oldfield E (1994) Growth inhibition, tumor maturation, and extended survival in experimental brain tumors in rats treated with phenylacetate. Cancer Res 54:2923–2937
3. Samid D, Shack S, Sherman L (1992) Phenylacetate: a novel nontoxic inducer of tumor cell differentiation. Cancer Res 52:1988–1992
4. Samid D, Shack S, Myers C (1993) Selective growth arrest and maturation of prostate cancer cells in vitro by nontoxic, pharmacological concentrations of phenylacetate. J Clin Invest 91:2288–2295
5. Samid D, Ram Z, Hudgins W, Shack S, Liu L, Walbridge S, Oldfield E, Myers C (1994) Selective activity of phenylacetate against malignant gliomas: resemblance to fetal brain damage in phenylketonuria. Cancer Res 54:891–895
6. Samid D, Yeh A, Prasanna P (1992) Induction of erythroid differentiation and fetal hemoglobin production in human leukemic cells treated with phenylacetate. Blood 80:1576–1581
7. Liu L, Shack S, Stetler-Stevenson W, Hudgins W, Samid D (1994) Differentiation of cultured human melanoma cells induced by the aromatic fatty acids phenylacetate and phenylbutyrate. J Invest Dermatol 103:335–340
8. Sidell N, Wada R, Han G, Chang B, Shack S, Moore T, Samid D (1995) Phenylacetate synergizes with retinoic acid in inducing the differentiation of human neuroblastoma cells. Int J Cancer 60:507–514
9. Brusilow S, Danney M, Waber L, Batshaw M, Burton B, Levitsky L, Roth K, Mckeethren C, Ward J (1984) Treatment of episodic hyperammonemia in children with inborn errors of urea synthesis. N Engl J Med 310:1630–1634
10. Simell O, Sipila I, Rajante J, Valle D, Brusilow S (1986) Waste nitrogen excretion via amino acid acetylation: benzoate and phenylacetate in lysinuric protein intolerance. Pediatr Res 20:1117–1121
11. Moldave K, Meister A (1957) Synthesis of phenylacetylglutamine by human tissue. J Biol Chem 229:463–476
12. James J, Smith R, Williams F, Reidenberg M (1972) The conjugation of phenylacetic acid in man, sub-human primates and non-primate species. Proc R Soc Lond B 182:25–35
13. Thibault A, Cooper M, Figg W, Venzon D, Sartor A, Tompkins A, Weinberger M, Headlee D, McCall N, Samid D, Myers C (1994) A phase I and pharmacokinetic study of intravenous phenylacetate in patients with cancer. Cancer Res 54:1690–1694
14. Thibault A, Samid D, Cooper M, Figg W, Tompkins A, Patronas N, Headlee D, Kohler D, Venzon D, Myers C (1995) Phase I study of phenylacetate administered twice daily to patients with cancer. Cancer 75:2932–2938
15. National Cancer Institute (1988) Guidelines for reporting of adverse drug reactions. Division of Cancer Treatment, National Cancer Institute, Bethesda, MD
16. Yamaoka K, Nakagawa T, Uno T (1978) Application of Akaike's information criterion (AIC) in the evaluation of linear pharmacokinetic equations. J Pharmacokinet Biopharm 6:165–175